Atomic Force Microscopy and Near-Field Scanning Optical Microscopy Measurements of Single Human Retinal Lipofuscin Granules

Christine M. R. Clancy,[†] Jeffrey R. Krogmeier,[‡] Anna Pawlak,[§] Malgorzata Rozanowska,[§] Tadeusz Sarna,[§] Robert C. Dunn,[‡] and John D. Simon*[,†,⊥]

Department of Chemistry, Duke University, Durham, North Carolina 27708; Department of Chemistry, University of Kansas, Lawrence, Kansas 66045; Institute of Molecular Biology, Jagiellonian University, Al. Mickiewicza 3, 31-120 Krakow, Poland; and Department of Biochemistry, Duke University Medical Center, Durham, North Carolina 27710

Received: August 24, 2000; In Final Form: October 25, 2000

Novel high-resolution microscopic techniques have been utilized to characterize the spatial distribution of orange emitting fluorophores, e.g., A2E, in lipofuscin granules isolated from human retinal pigment epithelium cells. Granules have been imaged using atomic force microscopy (AFM) and near-field scanning optical microscopy (NSOM). Near-field scanning optical microscopy images of lipofuscin show that the orange fluorophores, including A2E, are not major components of the granule. These results suggest that the orange fluorophores may not be the dominant photoactive species in lipofuscin.

1. Introduction

Lipofuscin is a generic name that is given to a heterogeneous group of complex fluorescent lipid−protein aggregates present in a wide variety of neuronal and nonneuronal tissues. In general, lipofuscin is formed in tissues with high oxidative stress (eye, heart, liver, brain, etc.). In the retinal pigment epithelium (RPE) of the human eye, lipofuscin is manifested as intracellular yellow-brown granules. This material in the RPE is thought to result from the lifelong accumulation of lysosomal residual bodies containing the end products of the phagocytosis of rod outer segments.[1−3] In fact, lipofuscin can occupy a considerable part of the cell volume in elderly people (up to 19% of the cytoplasmic volume by 80 years of age).[4] The structure and mechanism behind the accumulation of lipofuscin are not understood.

Lipofuscin has been proposed to be phototoxic to the RPE by acting as a source of reactive oxygen species.[5−8] The ability of lipofuscin to photogenerate reactive oxygen species under blue light exposure and thereby cause damage to the RPE has resulted in discussion of lipofuscin having a causal role in the development of age-related macular degeneration (AMD),[9−13,8] the major cause of blindness in people over the age of 60 in the western world.[14,15]

In a pioneering study of the emission properties of lipofuscin, Eldred and Katz isolated 10 fluorophores from chloroform extracts of RPE cells.[16] All fluorophores share a common absorbance peak lying between 280 and 330 nm, but only the orange-emitting fluorophores exhibit a second strong absorbance peak at 420 nm. This has led to the postulate that these latter species are involved in the blue-light-induced formation of reactive oxygen species.[6,7] In 1993, a pyridinium bis-retinoid, called A2E, was identified as being a major contributor to this orange fluorescence.[17] While its exact structure was not determined until 1996,[18] the isolation and identification of A2E has spurred an extensive research effort aimed at understanding its photochemical effects on retinal pigment epithelium cells. Studies have shown A2E to be phototoxic, suggesting that it is both a major hydrophobic component of lipofuscin[19] and is the dominant photoactive constituent under blue light excitation of lipofuscin.[20]

For photochemical activation of oxygen by lipofuscin to have detrimental effects in vivo, it is reasonable to postulate that the activation reactions occur on the surface of the lipofuscin granule. As a result, knowing the distribution of the orange fluorophores on or near the surface of the particle is important in assessing the role of these molecules in the oxygen activation process. The fact that A2E is easily extracted in chloroform solution without significant degradation of the granules suggests that this particular orange fluorophore is indeed located on or near the surface of the granules.[16] However, to date, the amount and distribution of any group of fluorophores on or within a lipofuscin granule have not been addressed. In this regard, there is no data that reveals how prevalent the orange-emitting fluorophores are in the lipofuscin granules. Experiments that address this issue shed light on the potential importance of these molecules in the photoreactivity of lipofuscin as well as the mechanism by which lipofuscin accumulation occurs in vivo. Herein we report experimental data collected using atomic force microscopy (AFM) and near-field scanning optical microscopy (NSOM). The goal of these experiments is to characterize the overall three-dimensional structural morphology and the corresponding distribution of orange-emitting fluorophores on or near the surface of lipofuscin granules.

The results presented here illustrate the unique capabilities of NSOM for probing into the distribution of chromophores within individual lipofuscin granules. The simultaneously collected topographical and emission near-field images allow for a direct comparison to be made between granule morphology and fluorescence. This leads to some surprising insights into both the distribution and extent of orange emitting fluorophores located in the lipofuscin granules. Moreover, unlike confocal

* Address correspondence to this author.
[†] Duke University.
[‡] University of Kansas.
[§] Jagiellonian University.
[⊥] Duke University Medical Center.

10.1021/jp0030544 CCC: $19.00
Published on Web 11/30/2000

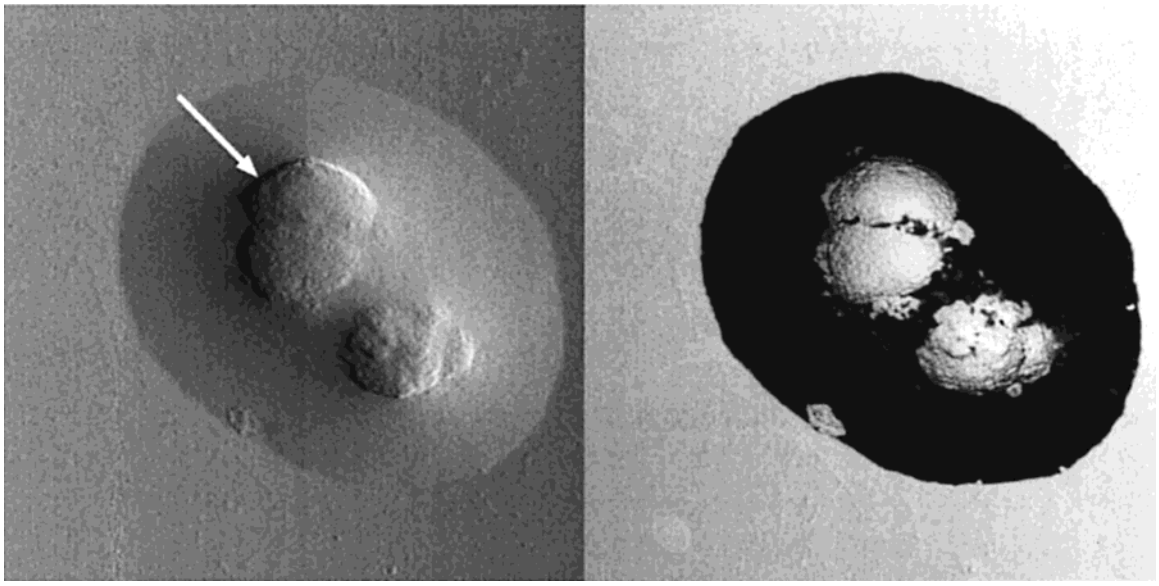

Figure 1. 3.50 μm × 3.50 μm AFM amplitude (left) and phase (right) images of an aggregate of lipofuscin granules deposited on a mica substrate. The amplitude image reveals that there is material deposited between the two granules.

microscopy, the spatial resolution in NSOM is not limited by diffraction effects. The increased spatial resolution of approximately 50−100 nm reveals structure in the granule fluorescence that was previously hidden in confocal measurements made in our laboratories.

2. Materials and Methods

Lipofuscin granules were isolated from human RPE cells from individuals 60−90 years old according to procedures previously described.[21] The granules were dispersed on a freshly cleaved mica surface by air-drying an aqueous lipofuscin solution. Height, amplitude, and phase measurements of the lipofuscin granules were taken using a Digital Instruments Nanoscope IIIa Bioscope AFM operated in tapping mode. Height data provides three-dimensional topographical information on the sample while the amplitude signal, which is the feedback error signal, is particularly sensitive to changes in sample height. Phase data, which measures the phase shift in the cantilever oscillation, responds to attractive and repulsive interactions between the AFM tip and the sample. Generally, this signal can be related to the stiffness of the sample and is useful for revealing domains that would otherwise be hidden in the height or amplitude images.

The simultaneous near-field fluorescence and force images were collected using a custom designed NSOM as described previously.[22] Briefly, the device is built on an inverted fluorescence microscope (Zeiss, Axiovert 135TV) and is operated using commercially available scanning probe electronics and software (Digital Instruments, Nanoscope IIIa), with only minor modifications made for near-field microscopy. Aluminum-coated near-field fiber optic probes are fabricated from 125 μm single-mode optical fiber (Newport) in either the straight geometry or cantilevered design using a micropipet puller (Sutter Instruments, P-2000) and a home-built evaporation chamber. For experiments utilizing straight near-field probes, a custom-designed near-field head is utilized to implement the shear-force feedback mechanism. For cantilevered probes, a commercial AFM head (Digital Instruments, Dimension) is utilized to implement a tapping-mode feedback scheme.

The sample is mounted directly beneath the tip on a closed loop $x-y$ piezo scanner (Mad City Labs, Inc.) that raster scans

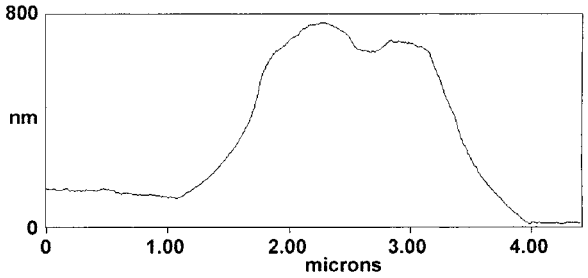

Figure 2. Profile of the height across the lipofuscin granules shown in Figure 1, taken along the direction of the arrow. This cross section reveals a significant amount of material deposited between the two granules.

the sample under the near-field tip. The appropriate line of an argon ion laser (Liconix, 5000 series) is passed through a $\lambda/2$ plate and $\lambda/4$ plate to control the polarization and is subsequently coupled into the fiber optic probe. Light exiting the near-field tip excites fluorescence in the sample which is collected from below with a high NA oil immersion objective (Zeiss, Fluar 40 × 1.3 NA). The residual excitation light is filtered (Chroma) and the collected fluorescence signal is imaged onto an avalanche photodiode detector (EG&G, SPCM-200). In the experiments reported herein, the 458 nm line from a continuous argon ion laser is used as the excitation source.

Images and data in Figures 1 and 2 are presented unprocessed. The NSOM topography images in Figure 3 (left) were plane-fit (first order) and flattened (zeroth order) so that the features in the images could be more clearly seen. However, this processing did not quantitatively or qualitatively alter the NSOM data.

3. Results and Discussion

Figure 1 shows amplitude and phase AFM images of an aggregate of lipofuscin granules deposited on a mica substrate. A profile of the height along the direction indicated by the arrow is shown in Figure 2. We find that lipofuscin granules have diameters on the order of one micron and heights ranging from 500 to 800 nm. The observed diameters are consistent with previous electron microscopy studies of lipofuscin granules.[16] In all cases, we observe material surrounding the granule that

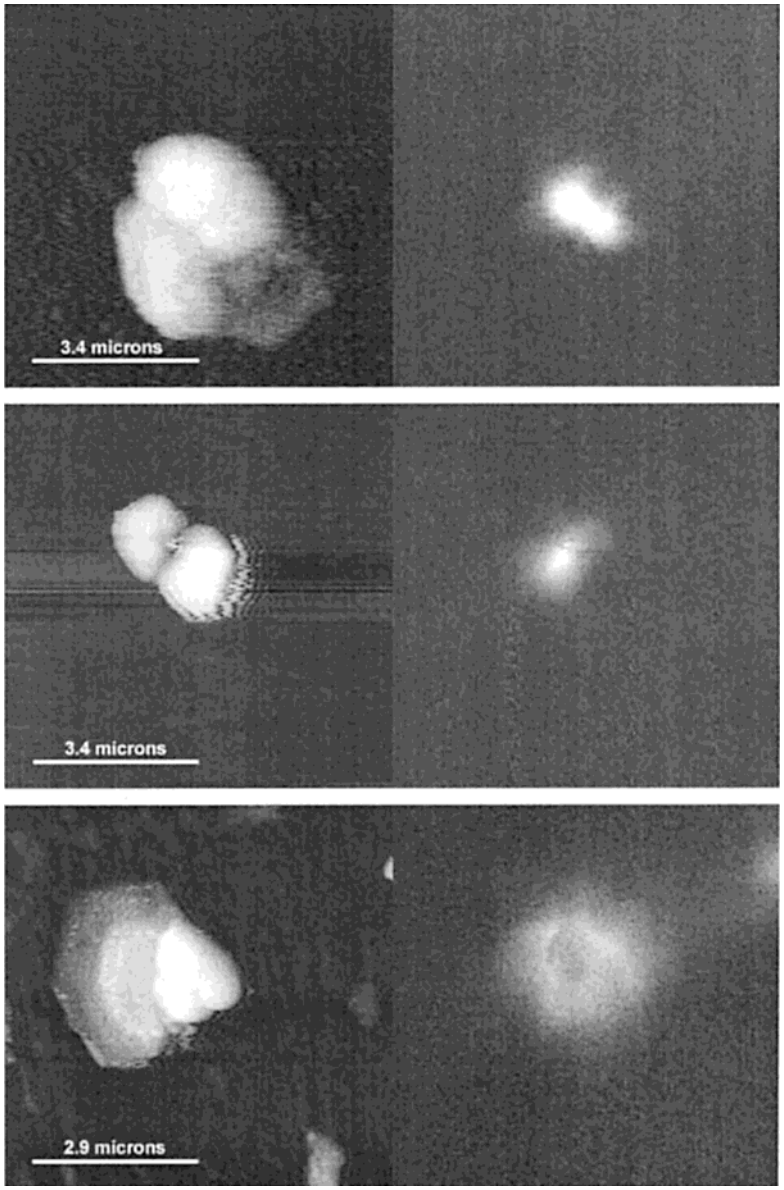

Figure 3. Simultaneously collected NSOM topography (left) and fluorescence (right) images of three different collections of lipofuscin granules demonstrating the range of structures observed. In the top pair of images, comparison of the topography and fluorescence data shows that only a small portion of the granules' surface is emissive. In the middle images, emission is observed at the junction of the two granules while the granules themselves are nonemissive. In the bottom pair of images, the granules are found to be weakly emissive with the region around the aggregate exhibiting much stronger emission in comparison to the granules.

has a distinctly different phase signal than the lipofuscin granules. This material clearly derives from the lipofuscin particle itself, as it is found only around lipofuscin particles and is also found welled up in the region between the granules. The nature of this material will be discussed below.

If the orange fluorophores present in lipofuscin were homogeneously distributed across the lipofuscin surface, the simultaneous NSOM fluorescence and topography images should directly correlate with one another. Figure 3 shows NSOM fluorescence and topography images for three different collections of lipofuscin granules that represent the range of behavior that we have observed. Following excitation at 458 nm, all granules examined using NSOM exhibit fluorescence signals that are significantly different from the simultaneously collected topography images.

The top pair of images in Figure 3 shows lipofuscin granules where only a small region on the surface of some of the granules emits light. For these granules in particular, less than 20% of the exposed surface area is emissive when excited at 458 nm. These images illustrate the utility of NSOM for these types of measurements. For example, a confocal image of this same area would imply that the granule size is $\sim$1.5 μm, the dimension of the fluorescent area, and not $\sim$3.5 μm, the size of the aggregate as shown in the NSOM topography image. AFM, on the other hand, can accurately report on the size of the granule but is unable to map the locations of the orange fluorophores. The middle pair of images display an aggregate of two lipofuscin particles where the granules themselves are nonemissive but the region at the interface of the two granules is emissive. The bottom pair of images reveal an aggregate of lipofuscin granules where the dominant emission is observed around the aggregate, with the granules being weakly emissive in comparison.

These images illustrate the range of results observed and are interesting with regard to both the structure of lipofuscin granules and the distribution of the orange emitting chromophores, including A2E. For the granules depicted in the two bottom pairs of images shown in Figure 3, emission from the region between and around the granules suggest that this region

was deposited during the drying process. The supernatant of the original lipofuscin suspension does not contain any orange-emitting fluorophores, so it is reasonable to conclude that this material was associated with the granules in the original suspension. This is further supported by the fact that we do not observe emission from regions on the mica where there are no lipofuscin granules. We postulate that upon evaporative drying, the lipid layer on the surface of the granules degrades and deposits material near the remaining granules. A2E is hydrophobic and so it is reasonable to assume that these fluorophores associate with the lipid layer. With the degradation of the lipid layer in the absence of the buffer solvent, these emissive molecules would deposit near the granules on the mica surface. This suggests that A2E is located on or near the surface of the lipofuscin granule and may not present to any extensive amount in the interior of the granule. This hypothesis is supported by phase images such as that shown in Figure 1, which show that a material very different from the lipofuscin granules both surrounds the granules and is collected between the granules. This material is the subject of ongoing work. Regardless, the data clearly reveal that the orange fluorophores are not homogeneously distributed throughout the granule.

It is important to note that although the NSOM images in Figure 3 show that most of the surface of the granule in not emissive, this does not mean that the dark areas of the lipofuscin granules are not absorbing incident radiation. It is possible that the dominant component of lipofuscin that leads to oxygen activation upon the absorption of blue light is not one of the orange fluorophores, but rather is a molecular constituent that is not emissive. Oxygen activation experiments that utilize NSOM to spatially select the region of the granule to be excited may address this question. Such experiments are currently being designed.

Acknowledgment. This work is support by Duke University and the Lord Foundation of North Carolina (J.D.S.), the Alfred P. Sloan Foundation (R.C.D.), NIH Dynamic Aspects of Chemical Biology Training Grant (J.R.K.), and the State Committee for Scientific Research (T.S.). We thank Dr. Janice M. Burke for providing the human retinal pigment epithelium cells.

References and Notes

(1) Feeney-Burns, L. *Curr. Top. Eye Res.* **1980**, *2*, 119−178.
(2) Feeney-Burns, L.; Hilderbrand, E. S.; Eldridge, S. *Invest. Ophthalmol. Visual Sci.* **1984**, *25*, 195−200.
(3) Sarna, T. *Photochem. Photobiol. B: Biol.* **1992**, *12*, 215−258.
(4) Weiter, J. J.; Delori, F. C.; Wing, G. L.; Fitch, K. A. *Invest. Ophthalmol. Visual Sci.* **1986**, *27*, 145−152.
(5) Gaillard, E. R.; Atherton, S. J.; Eldred, G.; Dillon, J. *Photochem. Photobiol.* **1995**, *61*, 448−453.
(6) Rozanowska, M.; Jarvis-Evans, J.; Korytowski, W.; Boulton, M. E.; Burke, J. M.; Sarna, T. *J. Biol. Chem.* **1995**, *270*, 18825−18830.
(7) Rozanowska, M.; Wessels, J.; Boulton, M.; Burke, J. M.; Rodgers, M. A. J.; Truscott, T. G.; Sarna, T. *Free Radical Biol. Med.* **1998**, *24*, 1107−1112.
(8) Winkler, B. S.; Boulton, M. E.; Gottsch, J. D.; Sternberg, P. *Mol. Vision* **1999**, *5*, U50−U60.
(9) Dorey, C. K.; Wu, G.; Ebenstein, D.; Garsd, A.; Weiter, J. J. *Invest. Ophthalmol. Visual Sci.* **1989**, *30*, 1691−1699.
(10) Eldred, G. E. *Gerontology* **1995**, *41*, 15−28.
(11) Katz, M. L.; Gao, C.-L.; Rice, L. M. *Mech. Ageing Dev.* **1996**, *92*, 159−174.
(12) Wassell, J.; Davies, S.; Bardsley, W.; Boulton, M. *J. Biol. Chem.* **1999**, *274*, 23828−23832.
(13) Wihlmark, U.; Wrigstad, A.; Roberg, K.; Brunk, U. T.; Nilsson, S. E. G. *AMPIS* **1996**, *104*, 265−271.
(14) Marshall, J. *Eye* **1987**, *1*, 282−295.
(15) Young, R. W. *Survey Ophthalmol.* **1987**, *31*, 291−306.
(16) Eldred, G. E.; Katz, M. L. *Exp. Eye Res.* **1988**, *47*, 71−86.
(17) Eldred, G. E.; Lasky, M. R. *Nature* **1993**, *361*, 724−726.
(18) Sakai, N.; Decatur, J.; Nakanishi, K.; Eldred, G. E. *J. Am. Chem. Soc.* **1996**, *118*, 1559−1560.
(19) Cubeddu, R.; Taroni, P.; Hu, D.-N.; Sakai, N.; Nakanishi, K.; Roberts, J. E. *Photochem. Photobiol.* **1999**, *70*, 172−175.
(20) Sparrow, J. R.; Nakanishi, K.; Parish, C. A. *Invest. Ophthalmol. Visual Sci.* **2000**, *41*, 1981−1989.
(21) Boulton, M. E.; Docchio, F.; Dayhaw-Barker, P.; Ramponi, R.; Cubeddu, R. *Vision Res.* **1990**, *30*, 1291−1303.
(22) Hollars, C. W.; Dunn, R. C. *Biophys. J.* **1998**, *75*, 342−353.